Muscle extracellular matrix degradation and contractibility following tendon rupture and disuse

Qia Zhang[1]
Sunil K. Joshi[1, 3]
Givenchy Manzano[1]
David H. Lovett[1, 2]
Hubert T. Kim[1, 3]
Xuhui Liu[1, 3]

[1] San Francisco Veterans Affairs (VA) Medical Center, San Francisco, California
[2] Department of Medicine, University of California at San Francisco, San Francisco, California
[3] Department of Orthopedic Surgery, University of California at San Francisco Sports Medicine and Shoulder Surgery, San Francisco, California

Corresponding author:
Xuhui Liu
San Francisco Veterans Affair (VA) Medical Center
4150 Clement Street, Building 2, Room 639
San Francisco, California 94121
e-mail: liux@orthosurg.ucsf.edu

Summary

Muscle extracellular matrix (ECM) plays an important role in maintaining muscular integrity and force transduction. However, the role of ECM in skeletal muscle atrophy remains unknown. In this study, we employed two clinically relevant mouse models of Achillotenotomy and hindlimb suspension to simulate Achilles tendon rupture and hindlimb disuse. The gastrocnemius was harvested following two weeks of treatment. We hypothesized that degradation of muscle ECM basement membrane lead to dysfunction of muscle contractility. Our results demonstrated a significant reduction of gastrocnemius single twitch force, isometric tetanic force, and contraction velocity following tendon rupture ($p<0.001$), but not disuse. Additionally, up-regulation of matrix metalloproteinase-2 (MMP-2) was observed only after tendon rupture ($p=0.00234$). These findings suggest that ECM remodeling and basement membrane degradation due to MMP-2 may be responsible for declined muscle contractibility. Inhibiting ECM degradation enzymes may be a potential treatment strategy for skeletal muscle atrophy after tendon rupture.

KEY WORDS: Achillotenotomy, basement membrane, extracellular matrix, hindlimb suspension, matrix metalloproteinase-2, muscle atrophy.

Introduction

Skeletal muscle atrophy, defined as the reduction of muscle mass, impacts patients recovering from surgery, injury, and immobility. It is a serious condition that produces significantly weaker musculature ensuing in adverse functional consequences[1], leading to a diminished muscle force generation.

Patients undergoing limb disuse are highly susceptible to developing muscle wasting diseases. The cause-and-effect relationship between limb unloading and disuse atrophy has been identified[2]. Limb immobilization, including wheelchair confinement, bed rest, and external casts all result in a loss of muscle mass. A disuse period as short as one week can result in a net reduction of muscle weight and protein synthesis[3-5]. Although the exact mechanism is unknown, a possible pathway responsible for muscle weight loss after disuse is the ubiquitin-proteasome protein degradation[6, 7].

Muscle atrophy following tendon rupture is another common complication seen by other physicians in addition to orthopaedic surgeons. Although previous studies have outlined detailed biochemical and histological properties of tendons after tendon rupture and some of these findings have been incorporated into the clinical realm, little is known regarding the mechanical response of muscles to tendon injury[8, 9].

Previous studies, including our own, have indicated that the skeletal muscle extracellular matrix (ECM) plays a critical role in muscle atrophy induced by tendon rupture[10]. The ECM forms a complex architecture that not only integrates mechanical signals, but also stores them to ensure optimal force transmissions[11-14]. There has been a growing body of evidence showing that ECM participates in fiber force transduction, maintains muscle normal function, and affects a muscle's ability to adapt to disease and injury[15, 16]. One important component of the ECM is the basement membrane, which mainly consists of type IV collagen and laminin. Interactions between components of the basement membrane provide a potential mechanism for lateral force transmission from myofibers. In our previous study, we have observed a significant reduction of collagen IV and laminin content with increased expression of a basement membrane degradation enzyme-matrix metalloproteinase-2 (MMP-2) in mouse gastrocnemius (GA) muscles after Achillotenotomy[17]. However, to our knowledge, there has not been a well-characterized study establishing the relationship between basement membrane degradation and muscle contractibility after tendon rupture.

The purpose of this study was to evaluate the relationship between basement membrane integrity and muscle contractility using two clinically relevant mouse atrophy mod-

els-Achillotenotomy (AT) and hindlimb suspension (HS). Our hypothesis was that basement membrane degradation, as mediated by MMP-2 leads to reduced muscle contractility in both AT and HS.

Materials and methods

Muscle Atrophy Mouse Models

This study was approved by our local Institutional Animal Care and Use Committee (IACUC). Thirty-six adult male mice (FVB/NJ strain) at 12 weeks were obtained from Charles River Laboratories Inc. Twelve mice underwent complete unilateral transection of the Achilles tendon. Contralateral sides served as non-treated control. The surgery followed the same procedures as described previously[17].

Twenty-four mice were used for the HS model. Twelve of these mice were suspended by the tails as described previously[18]. Twelve mice were kept in identical cages but without suspension as controls. Daily inspections were done for signs of possible tail lesions, discoloring, or discomfort.

Muscle Biomechanical Testing

All mice underwent *in situ* muscle functional testing on GA muscles 2 weeks after surgery/suspension. The Achilles tendon was exposed and attached to a force transducer (Grass Tech FT03 Transducer, Astro-Med Inc) by using a 4-0 suture silk. The femur was securely clamped and fixed to the table. A bipolar electrode was inserted through the sciatic nerve to stimulate muscle contraction. Animals were under isoflurane anesthesia during the entire procedure, and maintained at an ambient temperature of 30° C using a heating lamp. Every measurement was preceded by 2 minutes of rest to allow muscle relaxation before new stimulations. Single pulse stimuli (12 V, 0.02 sec duration) were applied with 0.5 mm increments of muscle-tendon length to establish optimum twitch force. Tetanic contractions were achieved by stimulating the sciatic nerve with a train of pulses with supramaximal stimulus intensity (12 V, 0.5 sec duration, 100-180 Hz). The frequency of train pluses was adjusted in 20 Hz increments until the maximum isometric tetanic force was obtained. Twitch velocity was calculated as the rate at which single pulses were generated over a unit time. Data was acquired through Poly View 16 program (Grass Tech, Astro-Med Inc.) at a sampling rate of 4000 Hz.

Muscle Harvesting

Immediately following muscle mechanical testing, all mice from AT and HS groups were sacrificed. GA muscles were harvested and the remaining tendon was removed at the muscle-tendon junction. The wet weight of the muscle was measured immediately[17]. Muscle was divided transversely into halves for histological and biological analysis.

Histology

Muscle samples were mounted on cork discs with 10% w/v tragacanth gum (Sigma-Aldrich Inc.) in water and flash frozen in liquid nitrogen-cooled isopentane[17]. They were then cyro-sectioned at -20º C at a thickness of 10 μm. Only sections at the bellies of the muscles were used for histological analysis. Sections were stained with Masson's Trichrome Kit for connective tissue (FisherSci Inc.) using manufacturer's instructions. Muscle fiber cross-sectional area was determined using Image J Software (NIH). Five hundred fibers in each muscle sample were calculated in the mid-section of gastrocnemius bellies, with a total of four samples chosen randomly (2,000 fibers total) for measurement analysis as described previously[19].

Immunofluorescence Staining

Immunofluorescence staining was performed for type IV collagen and laminin. Representative frozen cross sections were incubated with an anti-type IV collagen monoclonal antibody (1:2,000, Abcam Inc.) and anti-laminin monoclonal antibody (1:25, Sigma-Aldrich Inc.) at 4° C overnight. Sections were then incubated with rhodamine conjugated secondary antibody (Santa Cruz Biotechnology Inc.) for 1 hour at room temperature in the dark on the following day. Pictures of the samples were taken with a camera attached to a fluorescence microscope (Zeiss Axiovert 200 M, Zeiss Inc.) with constant exposure time. The intensity of fluorescence was measured using Image J software to compare the relative intensity of fluorescence between samples as described previously[20].

Reverse Transcription Polymerase Chain Reaction (RT-PCR).

Total RNA was isolated using Trizol reagent (Invitrogen Inc.) according to manufacturer's instructions. Isolated RNA was quantified and normalized to synthesize cDNA using a Transcriptor First Strand cDNA Synthesis Kit (Roche Applied Bioscience Inc.). RT-PCR was performed to quantify the expression of MMP-2 in our muscle samples using a Light Cycler 480 SYBR Green I Master kit (Roche Applied Bioscience) on a Prism 7900HT detection system (Applied Biosystems Inc.) with MMP-2 primers: (forward) 5'-GCCTCATACACAGCGTCAATCTT-3' and (reverse) 5'-CGGTTTATTTGGCGGACAGT-3'. MMP-2 gene expression was normalized to GAPDH: (forward) 5'TGCACCACCAACTGCTTAG-3' and (reverse) 5'-GGATGCAGGGATGATGTTC-3'.

Zymography

Total protein was isolated using tissue protein extraction reagent (T-PER, Pierce Biotechnology Inc.) according to manufacturer's instructions. Once protein levels were normalized, 60 μg of protein were loaded on 10% Novex®

Zymogram gels (Invitrogen Inc.). After an overnight incubation, the gels were stained with Simply Blue Safe Stain (Invitrogen Inc.) for 1 hour. Densitometric measurements were determined using Image J Software (NIH).

Statistical Analysis

For muscle weight and force analysis, a paired T-test was used to compare differences between the treatment and its control within each model. Statistical significance was defined as a p value of less than 0.05. Data was presented as the mean +/- standard deviation.

Results

There was no animal lost during or after surgery/suspension.

Muscle Wet Weight and Force Results

Significant GA wet weight loss was found after 2 weeks of AT and HS compared to their respective controls ($p<0.001$, Fig. 1 and Tab. 1). Significant GA single twitch force drop, isometric tetanic force drop, and twitch contraction velocity drop were only found in the AT model, but not in the HS model ($p<0.001$ for every comparison, Fig. 2 and Tab. 1).

Histological Analysis

Fiber anatomical cross-section area significantly decreased after two weeks of AT and HS compared to their respective controls ($p<0.001$, Fig. 4 and 5).

ECM Staining

Masson's Trichrome staining showed no notable change of total collagen content in treated and control muscles of both models (Fig. 3). However, significantly reduced fluorescence intensity of both laminin ($p=0.00182$) and collagen IV ($p=0.0177$) was observed only following 2 weeks of AT, not HS (Figs. 6-8).

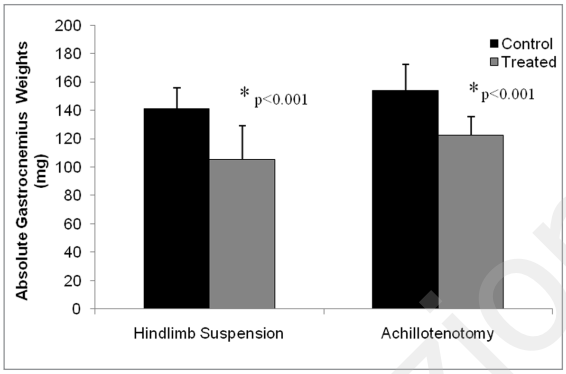

Figure 1. Comparison of gastrocnemius muscle weight between control and treatment groups following 2 weeks of hindlimb suspension and Achillotenotomy. Error bars represent standard deviation. *represents statistical significance (compared to the control group within each model).

MMP-2 RT-PCR and Zymography

MMP-2 mRNA expression was significantly up-regulated in GA muscles only after AT ($p<0.001$, Fig. 9). Zymography demonstrated that significant up-regulation of MMP-2 activities, both pro-enzymatic ($p=0.00949$) and activated ($p=0.00234$) forms, was seen only in the AT model (Fig. 10).

Discussion

The purpose of our current investigation was to evaluate the mechanical properties of GA following Achilles tendon rupture and hindlimb unloading via gross, functional, histological, and biochemical assessments. Our data showed that despite similar degrees of reduction in muscle weight and fiber cross-section area, muscle contractile properties

Table 1. Summary of muscle weight, force, and fiber cross-section area in both models.

	Hindlimb Suspension		Achillotenotomy	
	Control	Treated	Control	Treated
Sample Size (N)	12	12	12	12
Gastrocnemius Gross Outcomes				
Absolute Muscle Weight (mg)	154 ± 18	122 ± 13*	141 ± 15	105 ± 24*
Gastrocnemius Functional Outcomes				
Absolute Maximum Tetanic Force (mN)	1,782 ± 572	1,807 ± 580	1,946 ± 465	887 ± 439*
Absolute Single Twitch Force (mN)	308 ± 122	284 ± 70	415 ± 89	176 ± 95*
Single Twitch Force Produced per Unit Time (mN/sec)	11,744 ± 5,335	11,503 ± 3,611	11,847 ± 3,168	4,775 ± 1,898*
Gastrocnemius Histological Outcomes				
Muscle Fiber Cross Section Area (μm^2)	2,370 ± 832	1,515 ± 574*	2,151 ± 918	1,485 ± 706*

*** represents statistical significance ($p<0.001$, compared to the control group within each model).**

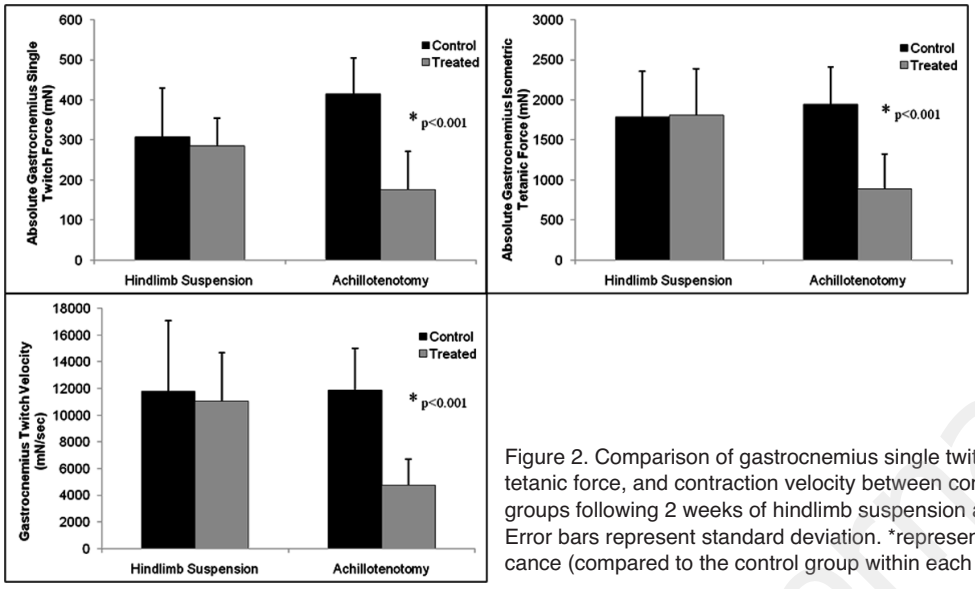

Figure 2. Comparison of gastrocnemius single twitch force, isometric tetanic force, and contraction velocity between control and treatment groups following 2 weeks of hindlimb suspension and Achillotenotomy. Error bars represent standard deviation. *represents statistical significance (compared to the control group within each model).

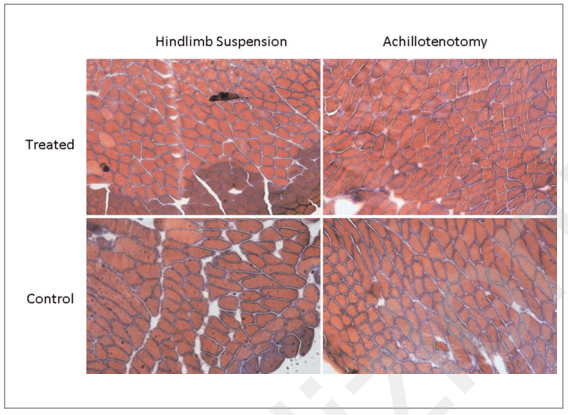

Figure 3. Typical images of Masson's Trichrome Staining (at 10x magnification) of gastrocnemius muscles in the control and treated groups after 2 weeks of hindlimb suspension/ Achillotenotomy.

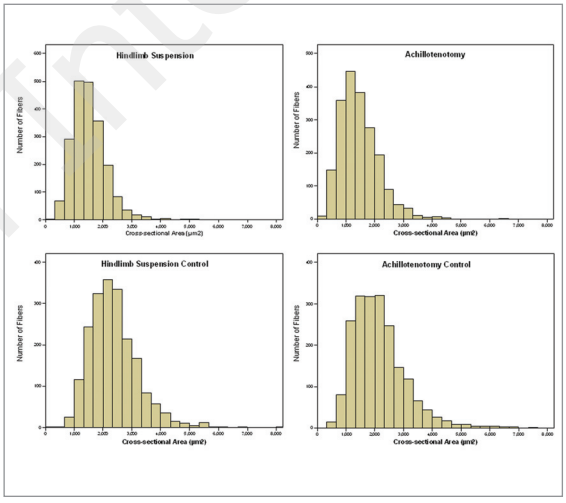

Figure 4. Histogram distribution of gastrocnemius anatomical fiber cross-section area of the control and treated groups after 2 weeks of hindlimb suspension/Achillotenotomy.

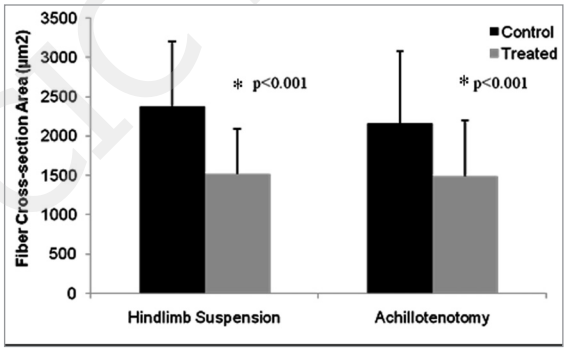

Figure 5. Comparison of gastrocnemius fiber cross-section area in control and treated groups after 2 weeks of hindlimb suspension/ Achillotenotomy. Error bars represent standard deviation. * represents statistical significance (compared to the control group within each model).

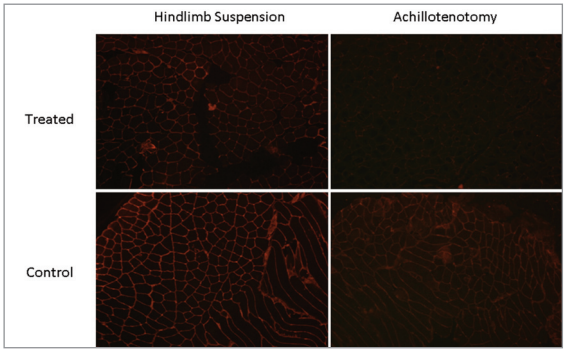

Figure 6. Typical images of immunofluorescence staining of type IV collagen (10x magnification) in the control and treated groups after 2 weeks of hindlimb suspension/Achillotenotomy.

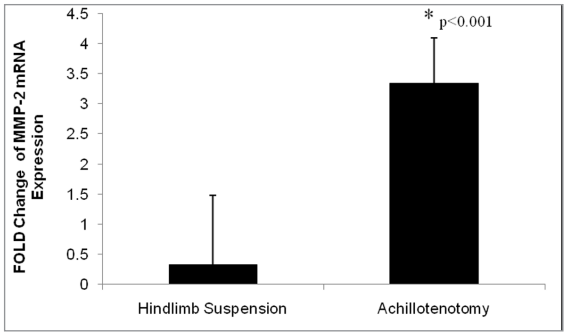

Figure 7. Fold change of MMP-2 mRNA expression following 2 weeks of hindlimb suspension and Achillotenotomy. Error bars represent standard deviation. *represents statistical significance (compared to the control group within each model).

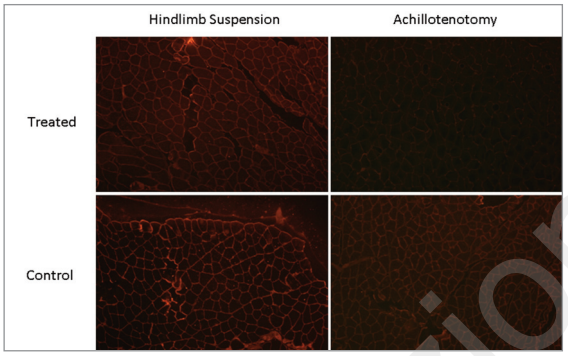

Figure 9. Typical images of immunofluorescence staining of laminin (10x magnification) in the control and treated groups after 2 weeks of hindlimb suspension/Achillotenotomy.

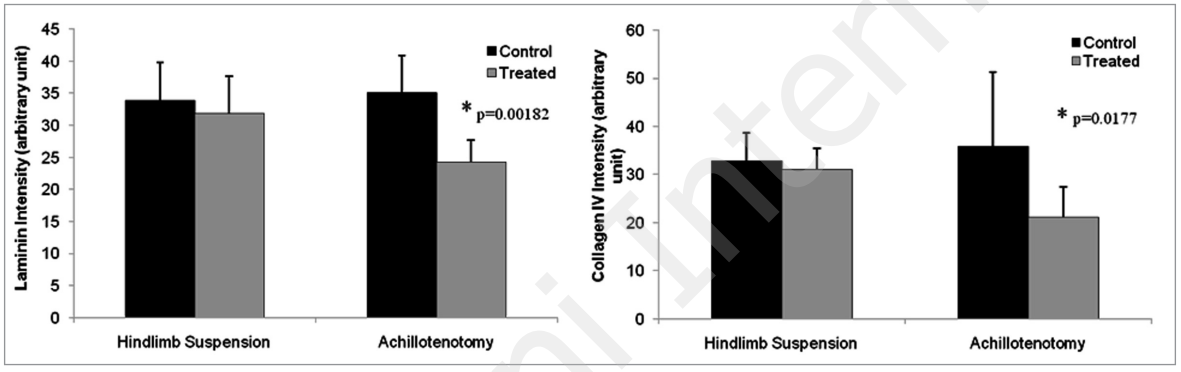

Figure 8. Semi-quantitative measurement of fluorescence intensity of laminin and type IV collagen staining of gastrocnemius muscles in the control and treated groups after 2 weeks of hindlimb suspension/Achillotenotomy. *represents statistical significance (compared to the control group within each model).

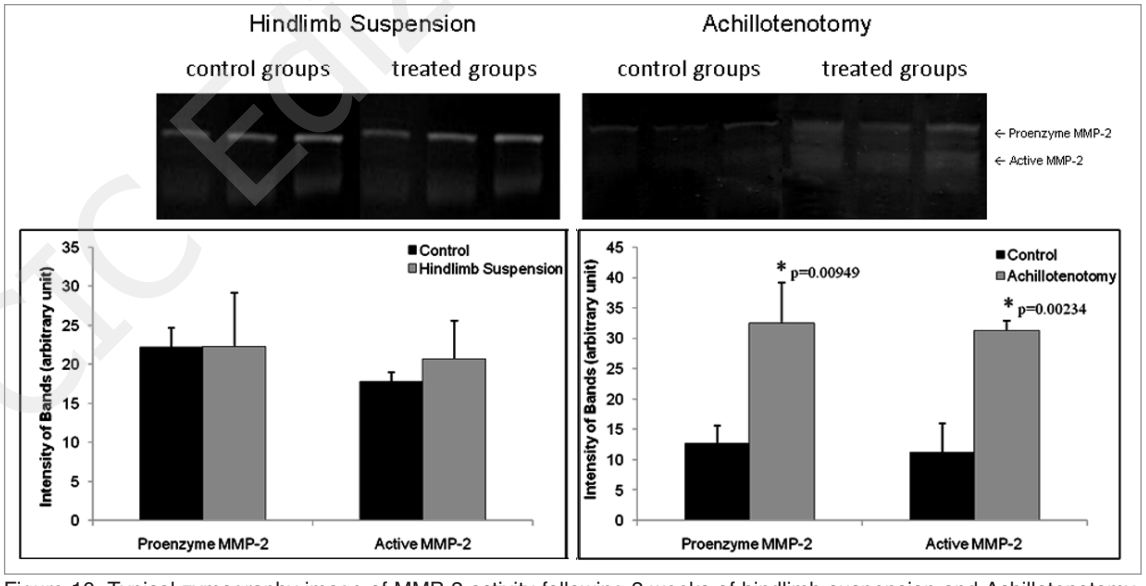

Figure 10. Typical zymography image of MMP-2 activity following 2 weeks of hindlimb suspension and Achillotenotomy. Semi-quantitative measurement of band intensity showed both pro- and active forms of MMP-2 were up-regulated in gastrocnemius muscles after Achillotenotomy, but not after hindlimb suspension. *represents statistical significance (compared to the control group within each model).

only significantly reduced in the AT model. These findings suggest that tendon rupture has a more profound influence on muscle biomechanics compared to disuse. Our data has important clinical implications when considering muscle contractility following tendon rupture as well as considering potential therapeutic modalities to alter the development of muscle atrophy following AT.

Based on our results, the reduction of GA wet weight was proportional to the reduction of fiber cross-section area, suggesting that muscle weight loss was mainly due to the reduction of muscle fiber size. Interestingly, *in situ* biomechanical testing demonstrated different functional outcomes between HS and AT models. In the HS group, single twitch force, tetanic force, and contraction velocity did not undergo significant change. Muscle contractibility was relatively preserved over the 2-week suspension period. However, in the AT model, muscle single twitch force and tetanic force dropped an average of 58% and 54%, respectively, compared to a 21% drop of wet weight. This discrepancy suggests that in addition to fiber size reduction, there may be different intrinsic mechanisms following tendon rupture and unloading disuse.

Since wet weight and fiber cross-section area dropped roughly the same percentage in both models, it is unlikely that the dramatic discrepancy of muscle mechanical function between both models was caused by the reduction of muscle fiber number and size. Though it accounts for only 1-10% of the skeletal muscle by mass[21, 22], the intramuscular connective tissue or the ECM has been known to play a critical role in organizing muscle fibers and ensuring its passive elastic response[23, 24]. While the Masson's Trichrome staining showed no apparent alteration of total collagen contents of GA between two atrophy models, immunofluorescence staining of the basement membrane did reveal that two of its major components-type IV collagen and laminin, were significantly degenerated after tendon rupture.

The alteration of basement membrane structure or components is a relatively under-investigated area in skeletal muscle research. It has been hypothesized for contributing to overall muscle strength and elasticity, although direct biophysical analysis is lacking[25]. The most abundant protein of the basement membrane is the triple-helical type IV collagen, while the major non-collagenous protein is laminin. Together they form distinct networks cemented by covalent cross-links of glycoprotein enactin/nidogen[26]. These components then bear a multitude of recognition sites that ultimately lead to the interaction with the cytoskeleton. The basement membrane may provide a significant fraction of the muscle tensile strength due to its complex association with reticular lamina, basal lamina, plasma membrane, and cytoskeleton[26-28].

MMP-2 is an ECM degrading enzyme tightly related to basement membrane remodeling. Collagen IV is a known substrate for MMP-2, which undergoes elevated expressions in various physiological and pathological events related to basement membrane metabolism, such as tissue repair, angiogenesis, and arterial enlargement[10, 29-32]. In our study, we found that MMP-2 expression and activity were only up-regulated in atrophic muscle after tendon rupture, not after suspension-induced disuse. In our previous study, we have shown that in MMP-2 knockout mice, collagen IV and laminin were relatively well preserved after AT[10]. This suggests that MMP-2 plays an important role in basement membrane degradation after tendon rupture.

It was surprising that muscle mechanical properties were largely preserved after 2 weeks of unloading disuse in spite of about 25% weight loss and fiber size reduction, suggesting that moderate amount of single fiber size reduction may not necessarily lead to muscle weakness at the gross level after a relatively short period of disuse. Fiber organization and force transmission are probably more important to muscle mechanical properties at the gross level.

There are several limitations to this study. First, a single time point of 2-week treatments was used for assessment. Previous work, including our own, has shown significant muscle atrophy at 2 weeks after AT and HS[17, 33]. Thus, we believe that 2 weeks is an appropriate time point for this study. However, longer time points will be considered in future studies. Secondly, it should be noted that "unloaded" muscles in our HS model were not completely "disused". The mice were allowed to move their legs in their daily activities, though they were non-weight bearing. Third, in this study, we only investigated a single muscle (GA), which consists of a combination of fast-twitched and slow-twitched fibers. Other muscles, especially relatively pure fast-twitched and slow-twitched muscles will be included in future studies. Finally, other measurements of muscle mechanical properties, such as muscle fatigue and stiffness, were not evaluated.

In summary, we report that a dichotomy exists between basement membrane degradation and muscle contractility following tendon rupture and disuse atrophy. Our findings suggest that the basement membrane plays an important role in maintaining muscle contractility. Preserving its integrity may be a direction in developing new therapeutic treatments of muscle atrophy.

Abbreviations

Achillotenotomy-AT.
extracellular matrix-ECM.
gastrocnemius-GA.
hindlimb suspension-HS.
matrix metalloproteinase-2-MMP-2.

Acknowledgements

This work was supported by the VA RR&D Merit Review Grant (RX000195). The authors thank Marissa Maimone for her assistance in muscle biomechanical testing.

References

1. Sandri M. Signaling in muscle atrophy and hypertrophy. Physiology (Bethesda). 2008; 23:160-170.
2. Zarzhevsky N, Carmeli E, Fuchs D, Coleman R, Stein H, Reznick AZ. Recovery of muscles of old rats after hindlimb immobilisation by external fixation is impaired compared with those of young rats. Exp Gerontol 2001; 36(1):125-140.
3. Goldspink DF. The influence of immobilization and stretch on protein turnover of rat skeletal muscle. J Physiol 1977; 264(1):267-282.

4. Booth FW, Seider MJ. Recovery of skeletal muscle after 3 mo of hindlimb immobilization in rats. J Appl Physiol 1979; 47(2):435-439.
5. Appell HJ. Muscular atrophy following immobilisation. A review. Sports Med 1990; 10(1):42-58.
6. Lecker SH, Goldberg AL, Mitch WE. Protein degradation by the ubiquitin-proteasome pathway in normal and disease states. J Am Soc Nephrol 2006; 17(7):1807-1819.
7. Jagoe RT, Goldberg AL. What do we really know about the ubiquitin-proteasome pathway in muscle atrophy? Curr Opin Clin Nutr Metab Care 2001; 4(3):183-190.
8. Jamali AA, Afshar P, Abrams RA, Lieber RL. Skeletal muscle response to tenotomy. Muscle Nerve 2000; 23(6):851-862.
9. Charvet B, Ruggiero F, Le Guellec D. The development of the myotendinous junction. A review. MLTJ 2012; 2(2):53-63.
10. Liu X, Lee DJ, Skittone LK, Natsuhara K, Kim HT. Role of gelatinases in disuse-induced skeletal muscle atrophy. Muscle Nerve 2010; 41(2):174-178.
11. Cukierman E, Pankov R, Stevens DR, Yamada KM. Taking cell-matrix adhesions to the third dimension. Science 2001; 294(5547):1708-1712.
12. Kjaer M. Role of extracellular matrix in adaptation of tendon and skeletal muscle to mechanical loading. Physiol Rev 2004; 84(2):649-698.
13. Grazi E. Experimental basis of the hypotheses on the mechanism of skeletal muscle contraction. MLTJ 2011; 1(3):77-84.
14. Maas H, Huijing PA. Myofascial force transmission between transferred rat flexor carpi ulnaris muscle and former synergistic palmaris longus muscle. MLTJ 2011; 1(4):127-133.
15. Gillies AR, Lieber RL. Structure and function of the skeletal muscle extracellular matrix. Muscle Nerve 2011; 44(3):318-331.
16. Ohlendieck K. Proteomic profiling of skeletal muscle plasticity. MLTJ 2011; 1(4):119-126.
17. Skittone LK, Liu X, Tseng A, Kim HT. Matrix metalloproteinase-2 expression and promoter/enhancer activity in skeletal muscle atrophy. J Orthop Res 2008; 26(3):357-363.
18. Turner RT, Morey ER, Liu C, Baylink D.J. Altered bone turnover during spaceflight. Physiologist 1979; 22(6):S73-S74.
19. Liu X, Laron D, Natsuhara K, Manzano G, Kim HT, Feeley BT. A mouse model of massive rotator cuff tears. J Bone Joint Surg Am 2012; 94(7):e41.
20. Roach DM, Fitridge RA, Laws PE, Millard SH, Varelias A, Cowled PA. Up-regulation of MMP-2 and MMP-9 leads to degradation of type IV collagen during skeletal muscle reperfusion injury; protection by the MMP inhibitor, doxycycline. Eur J Vasc Endovasc Surg 2002; 23(3):260-269.
21. Foidart M, Foidart JM, Engel WK. Collagen localization in normal and fibrotic human skeletal muscle. Arch Neurol 1981; 38(3):152-157.
22. Jarvinen TA, Jozsa L, Kannus P, Jarvinen TL, Jarvinen M. Organization and distribution of intramuscular connective tissue in normal and immobilized skeletal muscles. An immunohistochemical, polarization and scanning electron microscopic study. J Muscle Res Cell Motil 2002; 23(3):245-254.
23. Garfin SR, Tipton CM, Mubarak SJ, Woo SL, Hargens AR, Akeson WH. Role of fascia in maintenance of muscle tension and pressure. J Appl Physiol 1981; 51(2):317-320.
24. Knight PJ, Fortune NS, Geeves MA. Effects of pressure on equatorial X-ray diffraction from skeletal muscle fibers. Biophys J 1993; 65:814-822.
25. Tidball JG. Energy stored and dissipated in skeletal muscle basement membranes during sinusoidal oscillations. Biophys J 1986; 50(6):1127-1138.
26. Sanes JR. The basement membrane/basal lamina of skeletal muscle. J Biol Chem 2003; 278(15):12601-12604.
27. Sanes JR. Lineage tracing. The laatest in lineaage. Curr Biol 1994; 4(12):1162-1164.
28. Pisconti A, Bernet JD, Olwin BB. Syndecans in skeletal muscle development, regeneration and homeostasis. MLTJ 2012; 2(1):1-9.
29. Westermarck J, Kahari VM. Regulation of matrix metalloproteinase expression in tumor invasion. FASEB J 1999; 13(8):781-792.
30. Hudlicka O. Microcirculation in skeletal muscle. MLTJ 2011;1(1):3-11.
31. Buonocore D, Rucci S, Vandoni M, Negro M, Marzatico F. Oxidative system in aged skeletal muscle. MLTJ 2011; 1(3):85-90.
32. Rizzi R, Bearzi C, Mauretti A, Bernardini S, Cannata S, Gargioli C. Tissue engineering for skeletal muscle re generation. MLTJ 2012; 2(1):230-234.
33. Elder GC, McComas A.J. Development of rat muscle during short- and long-term hindlimb suspension. J Appl Physiol 1987; 62(5):1917-1923.